

## Preequilibrium $\gamma$ rays with angular momentum coupling

P. Obložinský

*Institute of Physics, Electro-Physical Research Centre of the Slovak Academy of Sciences,  
842 28 Bratislava, Czechoslovakia*

(Received 4 August 1986)

A spin-dependent expression is suggested for the emission rate of preequilibrium  $\gamma$  rays in the framework of the exciton model. The single-particle picture as well as the Brink-Axel hypothesis are adopted and the angular momentum coupling is treated in detail. The approach is consistent with the usual equilibrium  $\gamma$  emission rate and it also elucidates earlier nonspin preequilibrium results. The expression is completed by a fully spin-dependent formulation of the exciton model. As an illustrative example, the primary  $\gamma$  ray spectrum of the  $^{56}\text{Fe}(n,\gamma)$  reaction at 14.6 MeV is analyzed. The impact of the angular momentum conservation on the  $\gamma$  ray spectrum as well as the nucleon emission is rather small. The preequilibrium  $\gamma$  emission is dominated by  $\Delta n=0$  transitions between levels with low spins in the very first  $n$ -exciton stages of the reaction.

### I. INTRODUCTION

So far, only a few papers have dealt with the problem of preequilibrium  $\gamma$  ray emission,<sup>1-3</sup> in contrast with the attention given to other aspects of preequilibrium decay, particularly to nucleon as well as complex particle emission, intranuclear transitions, and particle-hole state densities. Physically, the problem of  $\gamma$  ray emission is limited to developing a proper emission rate. Preequilibrium  $\gamma$  rays seem to be predominantly of electric dipole character and they are due to single-particle transitions, implying the selection rule for the number of excitons  $\Delta n = -2, 0$ . Further, the Brink-Axel hypothesis must be taken into account and consistency with the equilibrium limit is desirable. In this sense the recent result of Akkermans and Gruppelaar,<sup>1</sup> which exhibits this consistency, seems more advantageous than that of Běták and Dobeš,<sup>2</sup> where the consistency is missing.

An essential limitation of the above works, however, is given by their complete neglect of the angular momentum coupling. One reason for it is that the angular momentum conservation in the preequilibrium models has rather generally been neglected. Another reason might be the complications with the principle of microscopic reversibility when applied to the preequilibrium  $\gamma$  ray emission. The point is that the emission is related to the transition  $n \rightarrow n, n-2$ , while the absorption proceeds via  $n \rightarrow n, n+2$ , or via  $n-2 \rightarrow n-2, n$ , and these processes are not simply reversible because of differences in the exciton quantum numbers of the respective initial and final states.

On the other hand, the basic techniques for the proper handling of the angular momentum coupling in the preequilibrium models have already been devised.<sup>4</sup> Also, the problems with the microscopic reversibility can be avoided by applying the golden rule of quantum mechanics as, for example, done by Liotta and Sorensen<sup>5</sup> in the equilibrium case. An important feature of our approach, however, is that we apply the golden rule to the inverse process too, and eliminate the matrix elements to get the

emission rate.

In the present paper we limit ourselves to the framework of the exciton model of nuclear reactions. Our main objective is to develop the spin-dependent formulation of the preequilibrium  $\gamma$  ray emission. The emission rate is derived in Sec. II and the spin-dependent formulation of the exciton model is completed in Sec. III. An illustrative example,  $^{56}\text{Fe}(n,\gamma)$  at 14.6 MeV, is examined in Sec. IV, and conclusions are given in Sec. V.

### II. PREEQUILIBRIUM $\gamma$ RAY EMISSION RATE

We consider an  $n$ -exciton level of energy  $E$  and spin  $J$  decaying by a  $\gamma$  ray emission with energy  $\epsilon$  and multipolarity  $\lambda$  which leads to a final level of energy  $U$  and spin  $S$ . First, we present the rate in its general form together with the energy structure for such a preequilibrium  $\gamma$  ray emission. Next, in this form our rate is compared with all earlier results. Then, we deal with angular momentum coupling. For the sake of clarity, we use the notation  $\lambda$  for multipolarity, though we consider electric dipole transitions only.

#### A. General form and energy structure

The  $\gamma$  ray emission rate per second per unit energy interval is

$$W_n^\gamma(EJ \xrightarrow{\epsilon\lambda} US) = \frac{2\pi}{\hbar} |\mathfrak{M}_n(EJ \xrightarrow{\epsilon\lambda} US)|^2 \omega_n(EJ \xrightarrow{\epsilon\lambda} US) \omega(\epsilon), \quad (1)$$

where  $|\mathfrak{M}_n|^2$  is the average squared transition matrix element and  $\omega_n$  is the density of the accessible final nuclear levels, while  $\omega$  refers to that of  $\gamma$  rays. These densities, together with the spin matrix element, will be evaluated explicitly, and the rest of the matrix element will be expressed by means of the inverse process, i.e., the  $\gamma$  ray absorption.

The quantity  $\mathfrak{M}_n$  is proportional to the reduced matrix element of a multipole electromagnetic operator that can be divided into radial and spin matrix elements.<sup>6</sup> Also, the nuclear level density can be, approximately, expressed as a product of energy and spin-dependent parts.<sup>4</sup> The single-particle nature of the electromagnetic operator<sup>7</sup> implies for the  $\gamma$  ray emission the selection rule  $\Delta n = -2, 0$  (Refs. 1 and 2). Thus, Eq. (1) leads to the two terms, in each of which the energy and spin parts are separated:

$$W_n^\gamma(EJ \rightarrow US) = \frac{2\pi}{\hbar} [ |\mathfrak{M}_n^{n-2}|^2 Y_n^{n-2} X_{nJ}^{n-2S} \omega(\epsilon) + |\mathfrak{M}_n^n|^2 Y_n^n X_{nJ}^{nS} \omega(\epsilon) ] . \quad (2)$$

Here,  $\mathfrak{M}_n^{n+\Delta n}$  is the nonspin part of the transition matrix element;  $Y_n^{n+\Delta n}$  represents the energy dependence of the density of accessible final nuclear levels, while  $X_{nJ}^{n+\Delta nS}$  contains the spin dependence of this density and the angular momentum structure of the transition matrix element. Finally,

$$\omega(\epsilon) = \frac{V}{\pi^2 \hbar^3 c^3} \epsilon^2 \quad (3)$$

is simply the state density of free  $\gamma$  rays, where  $V$  is the nuclear volume.

The rate of the inverse process per second can be expressed by means of the  $\gamma$  ray absorption cross section as  $c\sigma_n^{\text{abs}}/V$ , and also by using the golden rule. The single-particle operator leads now to the selection rule  $\Delta n = +2, 0$ ; therefore,

$$\frac{c}{V} \sigma_n^{\text{abs}}(US \rightarrow EJ) = \frac{2\pi}{\hbar} ( |\mathfrak{M}_n^{n+2}|^2 y_n^{n+2} x_{nS}^{n+2J} + |\mathfrak{M}_n^n|^2 y_n^n x_{nS}^{nJ} ) . \quad (4)$$

Here, the matrix elements refer to the transitions  $n \rightarrow n+2$  and  $n \rightarrow n$ , respectively, and the functions  $y$  and  $x$  have a similar meaning as  $Y, X$  in Eq. (2).

Equation (4) can be used to obtain the nonspin matrix elements. To this end an assumption should be made about the relation between the element associated with pair production and the element associated with the process  $\Delta n = 0$ . By assuming weak dependence on  $\Delta n$ , one gets

$$|\mathfrak{M}_n^{n+2}|^2 = |\mathfrak{M}_n^n|^2 , \quad (5)$$

implying that the branching ratio for the population of levels with different final exciton numbers due to absorption is fully given by the  $y$  and  $x$  functions.

Now we apply the Brink-Axel hypothesis to Eq. (4). In terms of the electric dipole  $\gamma$  ray strength functions of excited levels, the hypothesis is tantamount to assuming their identity with the  $\gamma$  strength function of the ground state (cf. p. 240 of Ref. 7). Thus, the strength function expressed via the photoabsorption cross section,

$$f_\gamma(\epsilon) = \frac{1}{\pi^2 \hbar^2 c^2} \frac{\sigma_n^{\text{abs}}(US \rightarrow EJ)}{g_J \epsilon} , \quad (6)$$

implies

$$\sigma_n^{\text{abs}}(US \rightarrow EJ) = \sigma_{\text{g.s.}}^{\text{abs}}(S \rightarrow \epsilon J) , \quad (7a)$$

with

$$\sigma_{\text{g.s.}}^{\text{abs}}(S \rightarrow \epsilon J) = \sigma_{\text{g.s.}}^{\text{abs}}(\epsilon) \frac{g_J}{3} , \quad (7b)$$

where  $g_J = (2J+1)/(2S+1)$  is the statistical factor and  $\sigma_{\text{g.s.}}^{\text{abs}}(\epsilon)$  is the full electric dipole photoabsorption cross section of a nucleus in the ground state. It can be expressed conventionally as

$$\sigma_{\text{g.s.}}^{\text{abs}}(\epsilon) = \sigma_R \frac{(\epsilon \Gamma_R)^2}{(\epsilon^2 - \Gamma_R^2)^2 + (E_R \Gamma_R)^2} , \quad (8)$$

with  $\sigma_R$ ,  $E_R$ , and  $\Gamma_R$  being the giant dipole resonance cross section, the energy, and the width, respectively.

The  $Y$  and  $X$  functions for emission are related to their counterparts for absorption, the  $y$  and  $x$  functions, by means of the detailed balance

$$(2J+1)\omega_n(E, J) Y_n^{n'} X_{nJ}^{n'S} = (2S+1)\omega_n(U, S) y_n^n x_{nS}^{nJ} , \quad (9)$$

where  $n' = n, n-2$  and  $\omega_n(E, J)$  is the total  $n$ -exciton level density.

Using Eqs. (2)–(5), (7), and (9), one gets the emission rate of preequilibrium  $\gamma$  rays in a rather general form,

$$W_n^\gamma(EJ \rightarrow US) = \frac{\epsilon^2 \sigma_{\text{g.s.}}^{\text{abs}}(\epsilon)}{3\pi^2 \hbar^3 c^2} \frac{\omega_{n-2}(U, S) b_{n-2S}^{nJ} + \omega_n(U, S) b_{nS}^{nJ}}{\omega_n(E, J)} , \quad (10)$$

where

$$b_{n-2S}^{nJ} = \frac{y_{n-2}^n x_{n-2S}^{nJ}}{y_{n-2}^n x_{n-2S}^{n-2J} + y_{n-2}^n x_{n-2S}^{nJ}} , \quad (11a)$$

$$b_{nS}^{nJ} = \frac{y_n^n x_{nS}^{nJ}}{y_n^n x_{nS}^{nJ} + y_n^{n+2} x_{nS}^{n+2J}} . \quad (11b)$$

The following relation holds,

$$b_{nS}^{n+2J} + b_{nS}^{nJ} = 1 , \quad (11c)$$

and analogous to the nonspin formulation of Akkermans and Gruppelaar,<sup>1</sup> the coefficients  $b_{nS}^{n+2J}$  and  $b_{nS}^{nJ}$  can be interpreted as the branching ratios that subdivide the photoabsorption cross section  $\sigma_n^{\text{abs}}$  over the different exciton levels accessible after absorption.

The particle-hole level density is written in a form with energy and spin separated,<sup>4</sup>

$$\omega_n(E, J) = \frac{g^{n+1} E^n}{p! h! (p+h-1)!} R_n(J) , \quad (12a)$$

$$R_n(J) = \frac{2J+1}{2\sqrt{2\pi}\sigma_n^3} e^{-(J+1/2)^2/2\sigma_n^2} , \quad (12b)$$

where  $g$  is the single-particle state density,  $n = p + h$ , and  $\sigma_n^2 = n\sigma^2$  is the spin cutoff parameter.<sup>8</sup> As shown in Ref. 9, the separation is justified provided the correction due to the Pauli principle is small, which, for example, is especially valid at low  $n$ .

The  $y$  functions, representing the energy part of the accessible level density after  $\gamma$  ray absorption, have a simple

form. Since the single-particle processes are involved,  $\Delta n = +2$  corresponds to a two-exciton state density, and  $\Delta n = 0$  corresponds to a one-exciton state density multiplied by the number of excitons available for the transition,

$$y^+ \equiv y_n^{n+2} = g^2 \epsilon, \quad (13a)$$

$$y^0 \equiv y_n^n = gn. \quad (13b)$$

### B. Comparison with previous results

Before we proceed with evaluating the  $x$  functions in the next subsection, it is worthwhile to compare our preequilibrium  $\gamma$  ray emission rate with the usual equilibrium expression, as well as with the nonspin preequilibrium rates obtained previously.

In the equilibrium limit the emission rate can be expressed as

$$W_{\text{eq}}^\gamma(EJ \rightarrow US) = \sum_n W_n^\gamma(EJ \rightarrow US) \frac{\omega_n(E, J)}{\omega(E, J)},$$

where  $\omega(E, J) = \sum_n \omega_n(E, J)$ . Inserting Eqs. (10) and (11c), we obtain

$$W_{\text{eq}}^\gamma(EJ \rightarrow US) = \frac{1}{h} \frac{\omega(U, S)}{\omega(E, J)} T_\gamma(\epsilon), \quad (14a)$$

where  $T_\gamma(\epsilon)$  is the  $\gamma$  ray transmission coefficient for the electric dipole transition,

$$T_\gamma(\epsilon) = \frac{2\epsilon^2 \sigma_{\text{g.s.}}^{\text{abs}}(\epsilon)}{3\pi \hbar^2 c^2} = 2\pi \epsilon^3 f_\gamma(\epsilon), \quad (14b)$$

in accord with the usual spin-dependent equilibrium emission rate (see, e.g., Grover<sup>10</sup>). This means that our preequilibrium rate satisfies the consistency requirement with the equilibrium result.

Our  $W_n^\gamma$  can be reduced to a nonspin expression provided all spin terms, i.e., the functions  $x$  and  $R$  in Eqs. (10)–(12), are adequately simplified. Assuming  $x=1$  and  $R \propto 2J+1$ , and summing Eq. (10) over the final spins  $S=J-1, J, J+1$ , we obtain the nonspin emission rate of Akkermans and Gruppelaar,<sup>1</sup> since Eqs. (11) and (13) give exactly their branching ratios,

$$b_{n-2}^n = \frac{g^2 \epsilon}{g^2 \epsilon + g(n-2)}, \quad b_n^n = \frac{gn}{g^2 \epsilon + gn}.$$

Our approach makes it possible to explain also the nonspin emission rate of Běták and Dobeš.<sup>2</sup> The latter differs from that of Ref. 1 by the coefficients

$$b_{n-2}^n = 1, \quad b_n^n = \frac{gn}{g^2 \epsilon}.$$

Equivalent to these coefficients is the assumption that the transition matrix element  $\mathfrak{M}_n$  in Eqs. (1) is independent of  $n$ . Then, Eq. (5) reads  $|\mathfrak{M}_n^{n+2}|^2 = |\mathfrak{M}_n^n|^2 = \text{const}$ , which can be obtained simply from Eq. (4) for  $n=0$ , i.e., for the ground state by realizing that for this state the absorption of the type  $\Delta n=0$  is not allowed.

As a consequence, Eq. (4) now implies, for the total photoabsorption cross section on a state  $n$ , that

$$\sigma_n^{\text{abs}}(U \rightarrow E) = \sigma_{\text{g.s.}}^{\text{abs}}(\epsilon) \left[ 1 + \frac{gn}{g^2 \epsilon} \right]. \quad (15)$$

Equation (15) means that the energy dependence of the photoabsorption cross section for the excited state differs in the functional form from that for the ground state. Following the Brink-Axel hypothesis, however, one should rather expect accordance of the two functional forms (cf. p. 240 of Ref. 7). Although the difference is small for low  $n$ , it may be of importance for larger  $n$ . Ultimately, as pointed out already in Ref. 1, it leads to the inconsistency between the emission rate of Ref. 2 and the usual equilibrium result.

### C. Angular momentum coupling

We evaluate the angular momentum coupling terms for the absorption,  $x_{nS}^{n+\Delta nJ}$ , adopting the approach outlined in a somewhat different context by Feshbach *et al.*<sup>4</sup> We consider the electric dipole transitions and discuss first the angular momentum structure of the reduced transition probability, after which we proceed with the averaging procedure.

The reduced transition probability

$$\frac{1}{2S+1} |\langle J || \mathcal{M}(\epsilon\lambda) || S \rangle|^2 \quad (16)$$

is determined by the reduced matrix element of the electric dipole operator  $\mathcal{M}(\epsilon\lambda)$ . We assume that the initial and final levels  $S, J$  are described by the same  $j_3$  core that does not change during the transition and by a single active excitation that makes the transition  $j_2 \rightarrow j_1$ ; see Fig. 1(a). The operator acts thus on this single exciton only. The reduced matrix element of such a system composed of two parts, with an unimportant phase factor omitted, is<sup>11</sup>

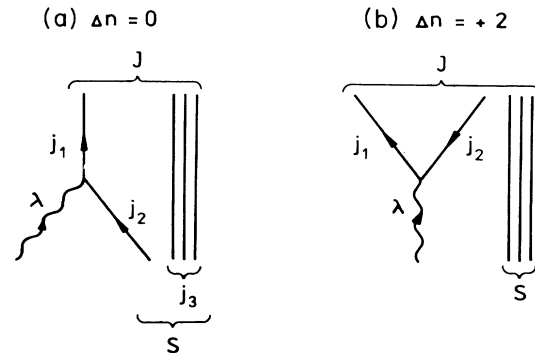


FIG. 1. Diagrams of  $x^0$  and  $x^+$  functions for  $\gamma$  ray absorption.

$$\langle (j_1 j_3) J || \mathcal{M}(\epsilon \lambda) || (j_2 j_3) S \rangle = [(2S+1)(2J+1)]^{1/2} \begin{Bmatrix} j_2 & j_3 & S \\ J & \lambda & j_1 \end{Bmatrix} \langle j_1 || \mathcal{M}(\epsilon \lambda) || j_2 \rangle, \quad (17)$$

where the single-particle electric dipole matrix element reads<sup>6</sup>

$$\langle j_1 || \mathcal{M}(\epsilon \lambda) || j_2 \rangle \propto [(2j_1+1)(2\lambda+1)(2j_2+1)]^{1/2} \begin{Bmatrix} j_2 & \lambda & j_1 \\ \frac{1}{2} & 0 & -\frac{1}{2} \end{Bmatrix}. \quad (18)$$

We substitute from Eqs. (17) and (18) into (16) and get the angular momentum structure of the reduced transition probability,

$$(2j_1+1)(2\lambda+1)(2j_2+1)(2J+1) \begin{Bmatrix} j_2 & \lambda & j_1 \\ \frac{1}{2} & 0 & -\frac{1}{2} \end{Bmatrix}^2 \begin{Bmatrix} j_2 & j_3 & S \\ J & \lambda & j_1 \end{Bmatrix}^2. \quad (19)$$

The reduced transition probability should be summed over final levels weighted by  $R_1(j_1)$  and averaged over initial levels. The averaging function is  $R_{n-1}(j_3)R_1(j_2)/R_n(S)$ , as can be shown in accordance with Ref. 4. Since for the  $\Delta n=0$  the particle-hole distinguishability has already been accounted for in calculating the energy function  $y^0$ , one has

$$x^0 \equiv x_{nS}^{nJ} = \frac{(2\lambda+1)(2J+1)}{R_n(S)} \sum_{j_1 j_2 j_3} (2j_1+1)R_1(j_1)(2j_2+1)R_1(j_2)R_{n-1}(j_3) \begin{Bmatrix} j_2 & \lambda & j_1 \\ \frac{1}{2} & 0 & -\frac{1}{2} \end{Bmatrix}^2 \begin{Bmatrix} j_2 & j_3 & S \\ J & \lambda & j_1 \end{Bmatrix}^2. \quad (20)$$

Equation (20) is substantially simplified for  $n=1$  since the core spin  $j_3$  is now fixed. Assuming  $j_3=0$ , one gets  $j_2=S, j_1=J$ ; hence the square of the 6- $j$  symbol is  $1/(2S+1)(2J+1)$ , and the averaging function is reduced to unity. Therefore,

$$x_{1S}^{1J} = (2\lambda+1)(2J+1)R_1(J) \begin{Bmatrix} S & \lambda & J \\ \frac{1}{2} & 0 & -\frac{1}{2} \end{Bmatrix}^2. \quad (21)$$

For the  $\Delta n=+2$  absorption, the above argument is slightly modified in view of Fig. 1(b). The 6- $j$  symbol in Eq. (19) is now replaced by

$$\begin{Bmatrix} 0 & S & S \\ J & \lambda & \lambda \end{Bmatrix}^2 = \frac{1}{(2S+1)(2J+1)},$$

the summation over final levels is weighted by  $R_1(j_1)R_1(j_2)$ , and the averaging over initial levels can be omitted. Thus,

$$x^+ \equiv x_{nS}^{n+2J} = \frac{2J+1}{2S+1} \sum_{j_1 j_2} (2j_1+1)R_1(j_1)(2j_2+1)R_1(j_2) \times \begin{Bmatrix} j_2 & j_1 & \lambda \\ \frac{1}{2} & -\frac{1}{2} & 0 \end{Bmatrix}^2 \Delta(S\lambda j), \quad (22)$$

where  $\Delta(S\lambda J)$  is 1 for  $|S-\lambda| \leq J \leq S+\lambda$  and 0 otherwise.

Provided our procedure is entirely consistent, the matrix elements as extracted from Eq. (4) should not depend on the angular momentum, and the whole spin dependence should be concentrated in the  $x$  functions. Thus, Eqs. (4) and (7) suggest that one should expect the following functional condition:

$$y^0 x^0 + y^+ x^+ \propto g_J = \frac{2J+1}{2S+1}. \quad (23)$$

That this condition is approximately valid can be seen by the following argument.

Equation (22) readily implies  $x^+ \propto g_J$  irrespective of  $n$ . Equations (20) and (21) after numerical evaluation suggest that although  $x^0$  is not strictly proportional to  $g_J$  at low  $n$ , it approaches this condition well at larger  $n$ . The  $y$  functions given by Eq. (13) imply for preequilibrium  $\gamma$  rays  $y^+ \gg y^0$ , since low  $n$  and large  $\epsilon$  are involved; hence  $y^0 x^0 + y^+ x^+ \approx y^+ x^+ \propto g_J$ , as expected. The bulk of the equilibrium  $\gamma$  rays is of low energy, but it originates from

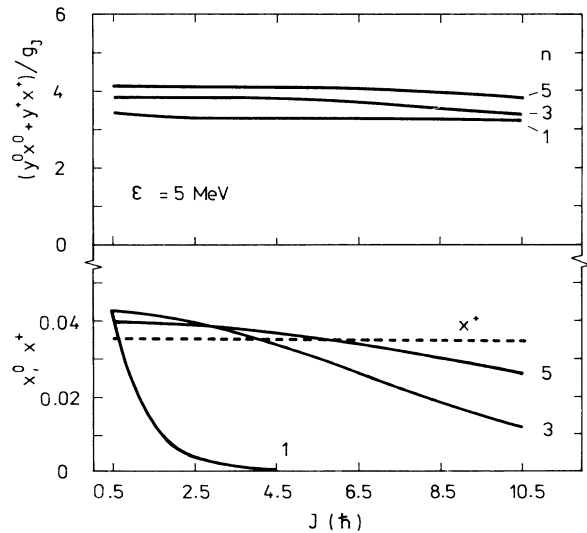


FIG. 2. Dependence of  $x$  functions on the angular momentum calculated for absorption of  $\gamma$  rays on  $^{57}\text{Fe}$  assuming  $S=J$ . Shown below are  $x^0$  for  $n=1,3,5$  and  $x^+$ , which is constant. Shown above is the corresponding function  $(y^0 x^0 + y^+ x^+) / g_J$  for the  $\gamma$  ray energy  $\epsilon=5$  MeV.

larger  $n$ ; therefore the condition (23) should again be approximately satisfied.

As an example we have studied the  $^{56}\text{Fe}(n,\gamma)$  reaction at the incident neutron energy 14.6 MeV; see Sec. IV. Here, in Fig. 2, we show  $x^0$  as a function of  $J$  for the intermediate statistical factor  $g_J=1$ . It is seen that  $x^0$ , with increasing  $n$ , becomes really spin independent. Furthermore, shown in Fig. 2 is the corresponding function  $(y^0x^0+y^+x^+)/g_J$ . Again, it is seen that even for a relatively low  $\gamma$  ray energy  $\epsilon=5$  MeV, this function is, within a few percent, constant.

### III. THE EXCITON MODEL WITH ANGULAR MOMENTUM COUPLING

The closed-form expression for the differential cross section of a, say,  $(b,\gamma)$ , reaction can be written in the never-come-back approximation of the exciton model as

$$\frac{d\sigma_{(b,\gamma)}(\epsilon)}{d\epsilon} = \sum_J \sigma_b(E,J) \sum_{\substack{n=1 \\ \Delta n=2}} \left[ \prod_{k=1}^{n-2} \frac{\Gamma_{kJ\downarrow}}{\Gamma_{kJ}} \right] \sum_s \frac{W_n^\lambda(EJ \rightarrow US)}{W_{nJ}}, \quad (24)$$

where  $\sigma_b(E,J)$  is the composite-nucleus cross section, the term in large parentheses is the depletion factor, and  $W_{nJ}, W_n^\lambda$  is the total decay rate and the channel emission rate, respectively. The damping and the total widths are given as

$$\Gamma_{nJ\downarrow} = \hbar W_{nJ\downarrow}, \quad (25a)$$

$$\Gamma_{nJ} = \hbar W_{nJ\downarrow} + \sum_\nu \hbar \sum_S \int W_n^\nu(EJ \rightarrow US) d\epsilon, \quad (25b)$$

where  $W_{nJ\downarrow}$  is the damping (intranuclear) transition rate of the type  $\Delta n = +2$ , and  $W_n^\nu$  is the nucleon emission rate,  $\nu$  being a neutron or a proton.

Nucleon emission in the exciton model is treated as the single-particle process  $n \rightarrow n-1$ . The emission rate can be readily obtained by considering the angular momentum conservation and by applying detailed balance.<sup>12</sup> If one further distinguishes neutrons and protons, the emission rate reads<sup>13</sup>

$$W_n^\nu(EJ \rightarrow US) = \frac{1}{h} \frac{\omega_{n-1}(U,S)}{\omega_n(E,J)} Q_\nu(n) \times \sum_{j=|S-1/2|}^{S+1/2} \sum_{l=|J-j|}^{J+j} T_l(\epsilon), \quad (26)$$

$T_l(\epsilon)$  being the transmission coefficient and  $Q_\nu(n)$ , as expressed in Ref. 14, represents the fraction of neutrons or protons among excited particles.

We evaluate the damping transition rate in a way close to the usual nonspin approach. The residual interaction involved is the two-body scattering of the type  $n \rightarrow n+2$ . Because of (12) the energy and the angular momentum dependence can be factorized and the golden rule written as

$$W_{nJ\downarrow} = \frac{2\pi}{\hbar} |M_n^{n+2}|^2 Y_{n\downarrow} X_{nJ\downarrow}, \quad (27)$$

where  $|M_n^{n+2}|^2$  is the average squared nonspin part of the intranuclear transition matrix element,  $Y_{n\downarrow}$  is the energy part of the accessible final levels (see, e.g., Ref. 15),

$$Y_{n\downarrow} = \frac{g^3 E^2}{2(n+1)}, \quad (28)$$

and  $X_{nJ\downarrow}$  determines all the angular momentum dependence of the process.

The function  $X_{nJ\downarrow}$  can be evaluated exactly in the way devised for the multistep compound reactions in Ref. 4 and extended to the spin  $\frac{1}{2}$  particles in Ref. 16. By considering the residual two-body interaction in  $\delta$ -function form,

$$V(\mathbf{r}_1 - \mathbf{r}_2) = \text{const} \times \delta(\mathbf{r}_1 - \mathbf{r}_2),$$

and by applying standard techniques,<sup>17</sup> the angular momentum structure of the transition matrix element can be expressed as (see Fig. 3)

$$[(2j_5+1)(2j_3+1)(2j_1+1)(2j_2+1)]^{1/2} \times \begin{vmatrix} j_5 & j_3 & Q \\ \frac{1}{2} & 0 & -\frac{1}{2} \end{vmatrix} \begin{vmatrix} j_1 & j_2 & j_3 \\ \frac{1}{2} & -\frac{1}{2} & 0 \end{vmatrix} \Delta(Qj_4J), \quad (29)$$

where we neglected the unimportant phase factor. (The radial part of the transition matrix element was already incorporated into  $M_n^{n+2}$ , the average value of which is treated as parameter in the exciton model.) The matrix element (29) should be squared, averaged over initial states weighted by  $R_{n-1}(j_4)R_1(Q)/R_n(J)$ , and summed over final states weighted by  $R_2(j_3)R_1(j_5)$ . This latter procedure, finally, includes averaging over pair states weighted by  $R_1(j_1)R_1(j_2)/R_2(j_3)$ . The result is

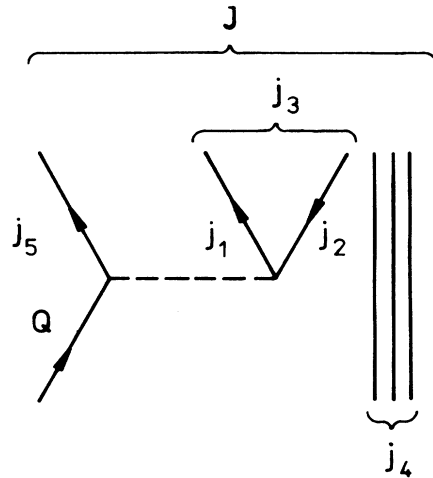


FIG. 3. Diagram of the  $X_{nJ\downarrow}$  function for damping.

$$X_{nJ\downarrow} = \frac{1}{R_n(J)} \sum_{j_4 Q} R_1(Q) \tilde{F}(Q) R_{n-1}(j_4) \Delta(Qj_4J), \quad (30)$$

where

$$\begin{aligned} \tilde{F}(Q) = & \sum_{j_3 j_5} (2j_5 + 1) R_1(j_5) (2j_3 + 1) \\ & \times F(j_3) \begin{vmatrix} j_5 & j_3 & Q \\ \frac{1}{2} & 0 & -\frac{1}{2} \end{vmatrix}^2, \end{aligned} \quad (31)$$

and the angular momentum density of pair states is

$$\begin{aligned} F(j_3) = & \sum_{j_1 j_2} (2j_1 + 1) R_1(j_1) (2j_2 + 1) \\ & \times R_1(j_2) \begin{vmatrix} j_1 & j_2 & j_3 \\ \frac{1}{2} & -\frac{1}{2} & 0 \end{vmatrix}^2. \end{aligned} \quad (32)$$

Equation (30) is simplified for a specific case  $n=1$ , since the core spin  $j_4$  is now fixed. Assuming  $j_4=0$ , one has

$$X_{1J\downarrow} = \tilde{F}(J). \quad (33)$$

An obvious question is how one should relate the non-spin part of the matrix element  $|M_n^{n+2}|^2$ , as introduced in Eq. (27), to the established systematics of the matrix elements  $|M_n|^2$  obtained from fits to nucleon spectra in earlier studies that, however, neglected the angular momentum conservation. We argue that the spectra evaluated in these studies should not be significantly influenced by the angular momentum effects. The reason is that neither the nucleon emission width nor the damping width depend strongly on the angular momentum (cf. Sec. IV). This, in turn, means that the matrix elements obtained earlier do take into account, on the average, the angular momentum part as well. Therefore, one should expect

$$|M_n^{n+2}|^2 \langle X_{nJ\downarrow} \rangle = |M_n|^2, \quad (34)$$

where the angular momentum term  $\langle X_{nJ\downarrow} \rangle$  is averaged over  $J$ .

The average squared matrix element  $|M_n|^2$  is often assumed to have  $n$ -independent form,  $|M_n|^2 = KA^{-3}E^{-1}$ , where  $K$  is the empirical constant.<sup>18</sup> More recent works<sup>19,20</sup> assume  $|M_n|^2$  increasing with  $n$ . Following Ref. 19, for example, one can set

$$\frac{2\pi}{\hbar} |M_n|^2 \frac{g^3 E^2}{2(n+1)} = \frac{1.4 \times 10^{21}}{k} E,$$

where the expression to the right is taken from the intranuclear transition rate adopted in the hybrid model, and the mean free path adjustment factor  $k$  is chosen so as to fit the usual rate at  $n=3$ . Considering  $g = \frac{1}{13}A$ , one thus gets

$$|M_n|^2 = \frac{n+1}{4} \frac{K}{A^3 E}. \quad (35)$$

It turns out that  $\langle X_{nJ\downarrow} \rangle$  depends on  $n$  only weakly. In our illustrative reaction  $^{56}\text{Fe} + n$  (14.6 MeV), for example,

we found  $\langle X_{nJ\downarrow} \rangle = 0.0208, 0.0208, \text{ and } 0.0207$  for  $n=3, 5, \text{ and } 7$ , respectively. The averaging was performed applying the distribution function given by the composite-nucleus cross section  $\sigma_b(E, J)$ . Taking simply the  $n=3$  value, one finally has

$$|M_n^{n+2}|^2 = \frac{n+1}{4 \langle X_{3J\downarrow} \rangle} \frac{K}{A^3 E}. \quad (36)$$

#### IV. ILLUSTRATIVE EXAMPLE

As an illustrative example we selected the  $^{56}\text{Fe}(n, \gamma)$  reaction at the neutron incident energy 14.6 MeV. The excitation energy, 22.0 MeV, sufficiently exceeds the giant dipole energy, 18.3 MeV, which, in turn, is 4 MeV above the strong tail from the  $\gamma$  rays produced by the  $(n, n'\gamma)$  processes. Thus, one should have a relatively large region of primary  $\gamma$  rays not affected by other components.

High energy  $\gamma$  ray spectra of this reaction were measured in Refs. 21 and 22. Cross sections reported in Ref. 21 go up to a  $\gamma$  ray energy of 18.5 MeV, displaying a kind of oscillation due to the unfolding procedure applied to the raw instrumental spectrum. The spectrum reported in Ref. 22, taken at a somewhat lower neutron energy of 14.1 MeV, is not unfolded. The spectrum, therefore, has remained smooth, but it is somewhat distorted by realistic energy resolution of the spectrometer, giving rise to energy points exceeding the full excitation energy. The two spectra can be regarded as complementary, with good accord in the overlapping  $\gamma$  ray energy region.

Calculations were performed with a set of fairly standard parameters. The single-particle state density was  $g = \frac{1}{13}A$  and, following Ref. 8, the spin cutoff parameter was taken as  $\sigma^2 = 0.28A^{2/3}$ . The intranuclear matrix element was taken with the constant  $K = 190 \text{ MeV}^3$  supported by the analysis of a number of double differential  $(n, n')$  cross sections at 14 MeV as performed in Ref. 23. The giant-dipole resonance (GDR)  $\gamma$  ray strength function was taken with the resonance parameters  $E_R = 18.3 \text{ MeV}$  (Ref. 24),  $\Gamma_R = 5 \text{ MeV}$ , and  $\sigma_R = 13A/\Gamma_R$  (in mb). The proton emission is weak and was neglected, and neutron transmission coefficients were obtained with the locally fitted optical potential.<sup>25</sup> The  $n=1$  state of the  $^{57}\text{Fe}$  composite nucleus corresponds to an excited neutron above the  $^{56}\text{Fe}$  ground state, implying zero core spin, as assumed in Eqs. (21) and (33). Simultaneously with the spin-dependent calculations, the nonspin calculations were performed for comparison.

Spin-dependent  $\gamma$  ray widths,

$$\Gamma_{nJ}^\gamma = \hbar \sum_S \int W_n^\gamma(EJ \rightarrow US) d\epsilon,$$

are compared with the non-spin values in Fig. 4. They indicate the importance of low spins in the preequilibrium  $\gamma$  emission. The results show that with increasing  $n$  the spin dependence of  $\Gamma_{nJ}^\gamma$  washes out and approaches non-spin widths. The widths for  $n=1$  are entirely due to the  $\Delta n=0$  term, since the  $\Delta n=-2$  process cannot take place there. At higher  $n$ , however, the role of this latter process increases until finally, at limiting values of  $n$ , it is practically the only process possible.

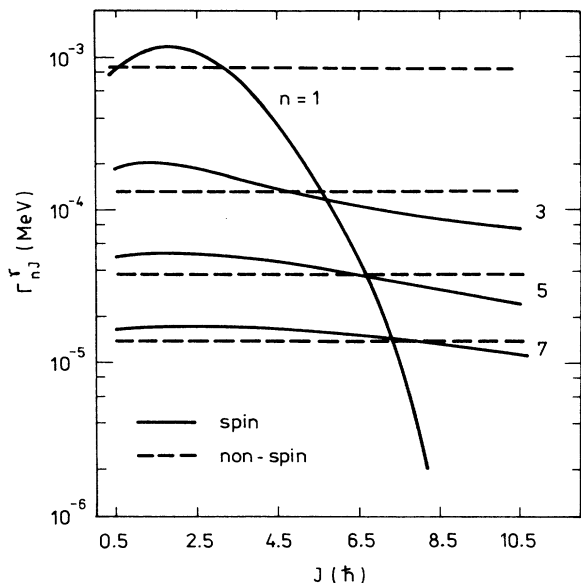


FIG. 4.  $\gamma$  emission width  $\Gamma_{nJ}^{\gamma}$  as a function of the angular momentum  $J$  for  $^{56}\text{Fe}(n,\gamma)$  at 14.6 MeV. Shown for comparison are nonspin widths.

Shown in Fig. 5 are neutron decay widths and damping widths,  $\Gamma_{nJ}^{\nu}$  and  $\Gamma_{nJ}\downarrow$ , as functions of the angular momentum. The neutron decay widths demonstrate their weak dependence on  $J$ . Nonspin neutron widths are not shown since in absolute terms they are nearly identical with the spin-dependent values. Damping widths, except for  $n=1$ ,

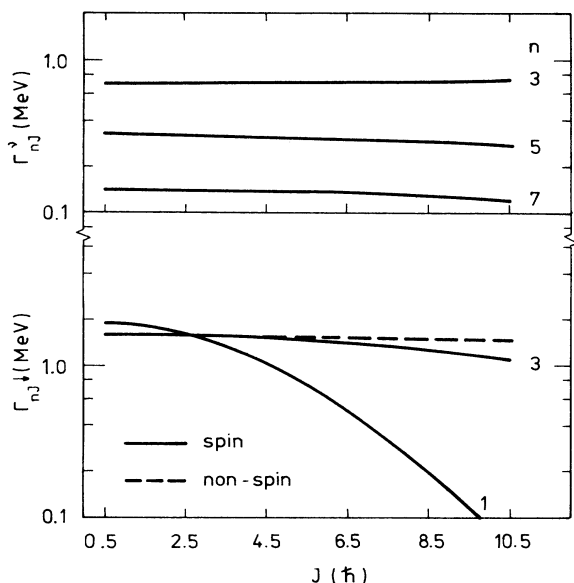


FIG. 5. Neutron decay width  $\Gamma_{nJ}^{\nu}$  and damping width  $\Gamma_{nJ}\downarrow$  as functions of the angular momentum for  $^{56}\text{Fe}(n,\gamma)$  at 14.6 MeV. Shown above is  $\Gamma_{nJ}^{\nu}$  for  $n=3,5,7$ . Shown below is  $\Gamma_{nJ}\downarrow$  for  $n=1,3$ , together with the nonspin width that is identical for all  $n$ .

depend on  $J$  only somewhat stronger than the corresponding neutron widths. With increasing  $n$  they approach the nonspin value that, in view of Eqs. (28) and (35), is constant for all  $n$ . Since neutron emission is governed by relative widths,  $\Gamma_{nJ}^{\nu}/(\Gamma_{nJ}\downarrow + \Gamma_{nJ}^{\nu})$ ,  $n \geq 3$ , our results imply weak impact of the angular momentum conservation on the preequilibrium neutron emission and, more generally, on the preequilibrium nucleon emission.

Shown in Fig. 6, finally, are the  $\gamma$  ray spectra. Of interest to us is the  $\gamma$  ray energy region 14–22 MeV, displaying a pure  $(n,\gamma)$  component. Below 14 MeV there is a strong increase in the observed cross sections due to the  $(n,n'\gamma)$  contribution. The curves show preequilibrium spectra of primary  $\gamma$  rays. The agreement with the data seems to be surprisingly good, especially if one notes that no adjustment of parameter has been made.

The  $n=1$  term, representing a kind of statistical description of direct capture, is shown separately. In this term the dominance of transitions involving low  $J$  is most clearly manifested. Thus, for example, the spin  $J=2.5$ , representing 16% of the composite-nucleus population, contributes to the  $n=1$  capture cross section by 25%, since the ratio  $\Gamma_{2.5}^{\gamma}/\Gamma_{1J}\downarrow = 6.9 \times 10^{-4}$ . For the spin  $J=6.5$ , however, this ratio is already down to  $0.86 \times 10^{-4}$  and the contribution to the  $n=1$  capture is only 1.4%, although the population of the composite nucleus amounts to 7.2%. The terms with higher  $n$  are more independent toward all spins, and with increasing  $n$  they gradually give rise to an increase of the low energy part seen in the full preequilibrium  $\gamma$  ray spectrum.

The impact of the angular momentum coupling on the shape of the  $\gamma$  ray spectrum is rather small. The nonspin result is somewhat higher than the spin one. This effect is basically due to the  $n=1$  term, where the  $\gamma$  ray emission from higher spins,  $J \geq 4.5$ , is suppressed most effectively. On the other hand, our parametrization of the intranuclear matrix element increases the  $n=1$  spin-dependent spectrum, since  $\langle X_{3J}\downarrow \rangle = 0.0208$  rather than  $\langle X_{1J}\downarrow \rangle = 0.0163$  was applied in Eqs. (36).

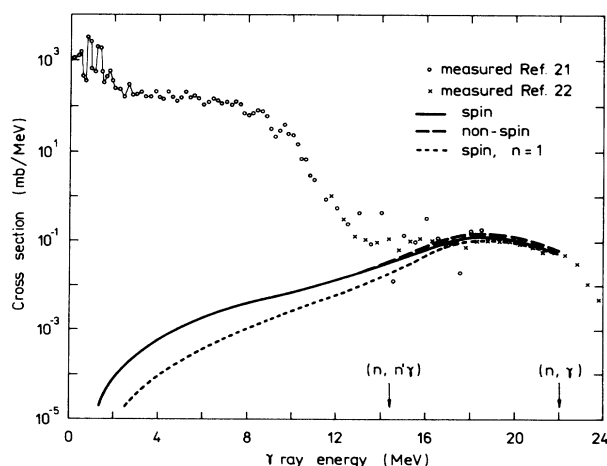


FIG. 6. Preequilibrium  $\gamma$  ray spectra as calculated for  $^{56}\text{Fe}(n,\gamma)$  at 14.6 MeV are compared with measured cross sections. Arrows mark the endpoint energies of  $\gamma$  rays.

The preequilibrium  $\gamma$  ray spectrum for  $^{56}\text{Fe}(n,\gamma)$  at 14.6 MeV reported in Ref. 26, supposedly based on the nonspin approach,<sup>2</sup> is an order of magnitude higher than our spectrum. We checked this point carefully. The calculation was repeated and we found that the spectrum in Ref. 26 was shifted by mistake by a factor of 10.

### V. CONCLUSIONS

We have derived the spin-dependent expression for the emission rate of the preequilibrium  $\gamma$  rays together with a fully spin-dependent formulation of the exciton model in the never-come-back approximation.

It seems that the impact of the angular momentum con-

servation on the  $\gamma$  ray spectra as well as on the nucleon emission is rather small. Essential in the preequilibrium  $\gamma$  ray emission are the lowest  $n$ -exciton levels, the  $\gamma$  transitions being presumably of the  $\Delta n=0$  type between levels with low angular momenta.

### ACKNOWLEDGMENTS

The author is grateful to S. Hlaváč for several valuable discussions. He wishes to thank E. Běták for carefully checking the calculations quoted in Ref. 26 and Š. Gmuka for calculating the neutron transmission coefficients. Careful reading of the manuscript by M. Blažek is gratefully acknowledged.

- 
- <sup>1</sup>J. M. Akkermans and H. Gruppelaar, *Phys. Lett.* **157B**, 95 (1985).
- <sup>2</sup>E. Běták and J. Dobeš, *Phys. Lett.* **84B**, 368 (1979).
- <sup>3</sup>V. A. Plyuyko and G. A. Prokopets, *Phys. Lett.* **76B**, 253 (1978).
- <sup>4</sup>H. Feshbach, A. Kerman, and S. Koonin, *Ann. Phys. (N.Y.)* **125**, 429 (1980).
- <sup>5</sup>R. J. Liotta and R. A. Sorensen, *Nucl. Phys.* **A297**, 136 (1978).
- <sup>6</sup>A. Bohr and R. R. Mottelson, *Nuclear Structure* (Benjamin, New York, 1969), Vol. 1, p. 387.
- <sup>7</sup>G. A. Bartholomew, E. D. Earle, A. J. Ferguson, J. W. Knowles, and M. A. Lone, *Adv. Nucl. Phys.* **7**, 229 (1973).
- <sup>8</sup>G. Reffo and M. Herman, *Lett. Nuovo Cimento* **34**, 261 (1982).
- <sup>9</sup>P. Obložinský, in *Proceedings of the 4th International Symposium on Neutron Induced Reactions, Smolenice, 1985*, edited by J. Kričtiak and E. Běták (Reidel, Dordrecht, 1986), p. 94.
- <sup>10</sup>J. R. Grover, *Phys. Rev.* **123**, 267 (1967).
- <sup>11</sup>A. Bohr and B. R. Mottelson, *Nuclear Structure*, Ref. 6, Vol. 1, p. 84.
- <sup>12</sup>P. Obložinský and I. Ribanský, *Nucl. Phys.* **A195**, 269 (1972).
- <sup>13</sup>H. Gruppelaar, in *Proceedings of the IAEA Advisory Group Meeting on Basic and Applied Problems of Nuclear Level Densities*, edited by M. R. Bhat, Brookhaven National Laboratory Report No. BNL-NCS-51694, 1983, p. 143.
- <sup>14</sup>C. Kalbach, *Z. Phys. A* **283**, 401 (1977).
- <sup>15</sup>P. Obložinský, I. Ribanský, and E. Běták, *Nucl. Phys.* **A226**, 347 (1974).
- <sup>16</sup>M. Herman, A. Marcinkowski, and K. Stankiewicz, *Nucl. Phys.* **A430**, 69 (1984); *Nucl. Phys.* **A435**, 859(E) (1985).
- <sup>17</sup>P. J. Brussaard and P. W. M. Glaudemans, *Shell-Model Applications in Nuclear Spectroscopy* (North-Holland, Amsterdam, 1977), Chap. 6.3.
- <sup>18</sup>C. Kalbach-Cline, *Nucl. Phys.* **A210**, 590 (1973).
- <sup>19</sup>J. M. Akkermans and H. Gruppelaar, *Z. Phys. A* **321**, 605 (1985).
- <sup>20</sup>C. Kalbach, *Phys. Rev. C* **32**, 1157 (1985).
- <sup>21</sup>S. Hlaváč and P. Obložinský, International Atomic Energy Agency Report No. INDC(CSR)-5/GI, 1983.
- <sup>22</sup>M. Budnar, F. Cvelbar, E. Hodgson, A. Hudoklin, V. Ivković, A. Likar, M. V. Mihajlović, R. Martinčić, M. Najžer, A. Perdjan, M. Potokar, and V. Ramšak, International Atomic Energy Agency Report No. INDC(YUG)-6/L, 1979.
- <sup>23</sup>J. M. Akkermans, H. Gruppelaar, and G. Reffo, *Phys. Rev. C* **22**, 73 (1980).
- <sup>24</sup>W. D. Myers, W.J. Swiatecki, T. Kodama, L. J. El-Jaick, and E. R. Hilf, *Phys. Rev. C* **15**, 2032 (1977).
- <sup>25</sup>E. D. Arthur and P. G. Young, in *Proceedings of the Symposium on Neutron Cross-Sections from 10 to 50 MeV*, edited by M. R. Bhat and S. Perlstein, Brookhaven National Laboratory Report No. BNL-NCS-51245, 1980, Vol. II, p. 731.
- <sup>26</sup>B. Basarragatscha, D. Hermsdorf, and E. Paffrath, *J. Phys. G* **8**, 275 (1982).